Journal of Chemistry and Technologies

pISSN 2663-2934 (Print), ISSN 2663-2942 (Online).

journal homepage: http://chemistry.dnu.dp.ua

UDC 547 + 544.18

DFT STUDY OF THE PHOTOCHEMICAL DIMERIZATION OF 3-HETEROARYL(FURYL, THIOPHYL, SELENOPHYL AND TELLUROPHYL)-ACRYLATES

Rezan Jalal, Hassan Hadi Abdallah*

Chemistry Department, College of education, Salahaddin University Erbil, 44001, Erbil, Iraq

Received 27 March 2021; accepted 2 June 2021; available online 20 July 2021

Abstract

Photochemical dimerization reactions provide an efficient approach to the synthesis of complex cyclobutene containing structures, which are often difficult to obtain by reactions of another type. Industrially, the photochemical healing of polymers proceeds successfully and very fast via [2+2] photocycloaddition. It is assumed that the heterocyclic ring has a great influence on the regioselectivity and stereoselectivity of photochemical dimerization of various heteroaryl acrylates. A detailed explanation of the observed photochemical reaction of different 3-heteroaryl(furyl, thiophyl, selenophyl and tellurophyl)-acrylates is furnished theoretically on the basis of a comprehensive review of the photochemical dimerizations of this type of compounds. Density functional theory (DFT) was used to study the reaction mechanism and locate all the intermediates and transition states along the potential energy curve. The calculated energy barriers were used to compare the stability of different conformations. The reactions showed good regio- and stereoselectivity through the formation of biradical transition state. The global electrophilicity, nucleophilicity, hardness, softness and ionization potential were evaluated to rationalize the results of the most stable isomers. In addition, IR vibration frequencies, energetic parameters and molecular orbital analysis were analyzed for the most stable products.

Keywords: Dimerization; DFT; 3-heteroaryl-acrylates; [2+2] cycloaddition.

ДОСЛІДЖЕННЯ ФОТОХІМІЧНОЇ ДИМЕРИЗАЦІЇ 3-ГЕТЕРОАРИЛ (ФУРИЛ, ТІОФІЛ, СЕЛЕНОФІЛ І ТЕЛУРОФІЛ)-АКРИЛАТІВ МЕТОДОМ DFT

Резан Джалал, Хассан Хаді Абдаллах

Хімічний факультет, Коледж освіти, Університет Салахаддіна в Ербілі, 44001, Ербіль, Ірак

Анотація

На основі всебічного огляду фотохімічних димеризацій різних 3-гетероарил(фурил, тіофіл, селенофіл і телурофіл)-акрилатів було представлено докладне теоретичне пояснення спостережуваної фотохімічної реакції сполук даного типу. Теорія функціоналу густини (DFT) була використана для вивчення механізму реакції і визначення місця розташування всіх проміжних і перехідних станів уздовж кривої потенційної енергії. Розраховані енергетичні бар'єри були використані для порівняння стабільності різних конформацій. Реакції показали гарну регіо - та стереоселективність за рахунок утворення бірадикального перехідного стану. Для обґрунтування результатів найбільш стабільних ізомерів було виконано порівняння значень глобальної електрофільності, нуклеофільності, жорсткості, м'якості і потенціалу іонізації. Крім того, для найбільш стабільних продуктів були проаналізовані частоти ІЧ-коливань, енергетичні параметри та виконаний аналіз молекулярних орбіталей.

Ключові слова: димеризація; DFT; 3-гетероарил-акрилати; [2+2] циклоприєднання.

**Corresponding author: e-mail: hassan.hadi.abdallah@gmail.com*

doi: 10.15421/jchemtech.v29i2.227788

Journal of Chemistry and Technologies, 2021, *29*(2), 240-253

ИССЛЕДОВАНИЕ ФОТОХИМИЧЕСКОЙ ДИМЕРИЗАЦИИ 3-ГЕТЕРОАРИЛ(ФУРИЛ, ТИОФИЛ, СЕЛЕНОФИЛ И ТЕЛЛУРОФИЛ)-АКРИЛАТОВ МЕТОДОМ DFT

Резан Джалал, Хассан Хади Абдаллах

Химический факультет, Колледж образования, Университет Салахаддина в Эрбиле, 44001, Эрбиль, Ирак

Аннотация

На основе всестороннего обзора фотохимических димеризаций различных 3-гетероарил(фурил, тиофил, селенофил и теллурофил)-акрилатов было представлено подробное теоретическое объяснение наблюдаемой фотохимической реакции соединений данного типа. Теория функционала плотности (DFT) была использована для изучения механизма реакции и определения местоположения всех промежуточных и переходных состояний вдоль кривой потенциальной энергии. Рассчитанные энергетические барьеры были использованы для сравнения стабильности различных конформаций. Реакции показали хорошую регио- и стереоселективность за счет образования бирадикального переходного состояния. Для обоснования результатов наиболее стабильных изомеров было произведено сравнение значений глобальной электрофильности, нуклеофильности, жесткости, мягкости и потенциала ионизации. Кроме того, для наиболее стабильных продуктов были проанализированы частоты ИК-колебаний, энергетические параметры, проведен анализ молекулярных орбиталей.

Ключевые слова: димеризация; DFT; 3-гетероарил-акрилаты; [2+2] циклоприсоединение.

Introduction

Photochemical dimerization reactions provide a very efficient approach to the synthesis of complex cyclobutane containing structures that are often difficult to synthesize by other reaction types [1; 2]. Cyclobutanes can undergo ring-expansion or fragmentation reactions [3]. The synthesis methods of four-membered carbocycles are limited compared to those available for the construction of five- and six-membered rings [4–6].

Natural products containing cyclobutane were obtained from a surprisingly diverse range of insect, microbial species, and plants [7–9]. Industrially, the photochemical healing of cracked and healed polymer samples proceeded successfully and very fast via [2+2] photocycloaddition which does not require any catalyst, additive, or severe heat treatment [10]. Indeed, there are numerous experimental and computational studies in the literature illustrating the importance of this type of reaction [11]. One of the oldest known photochemical dimerization was performed in 1902, when Chamichian published the results of the solid state photodimerization of cinnamic acid, coumarin, and stilbene [12; 13]. The solid state cinnamic acid was irradiated to produce the corresponding photodimers. Interestingly, the reaction products depend on the crystal form of the starting material, where the metastable β-form gives β-truxinic acid, while the stable α-form is reported to yield α-truxillic acid, as shown in Scheme 1 [13; 14].

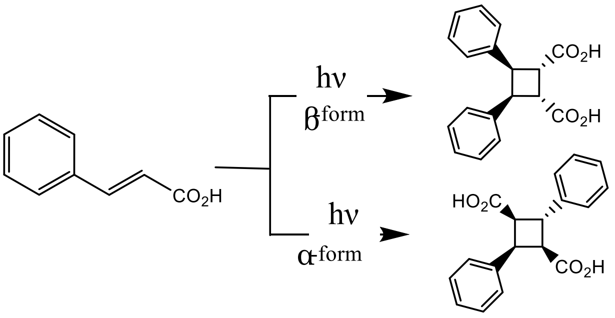

Scheme 1. The dimerization of cinnamic acid.

Similarly, the photochemical reaction of liquid ethyl cinnamate gave a mixture of two compounds with yields of 55 % and 25 %, respectively, Scheme 2 [15; 16].

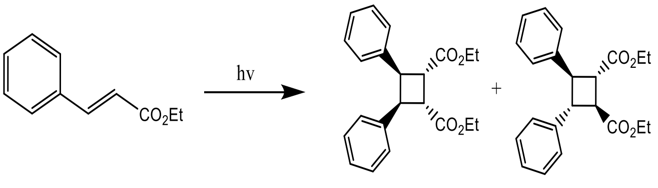

Scheme 2. The dimerization of ethyl cinnamate.

Irradiation of the mixture of methyl 3-(2-furyl)acrylate in acetonitrile and benzophenone as a sensitizer gave a mixture of two compounds with yields of 61 % and 27 % , respectively, Scheme 3 [17; 18].

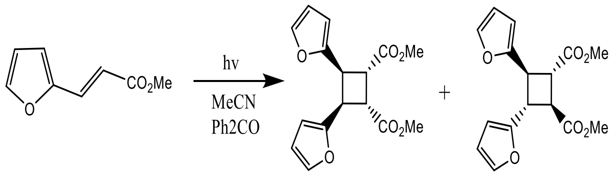

Scheme 3. The dimerization of methyl 3-(2-furyl)acrylate.

Based on the kinetic and spectroscopic properties, it was found that furylacrylate dimerization occurs in the triplet state of the molecule with a good stereoselectivity and a high regioselectivity [19; 20]. In addition, it was found that only head-to-head coupling was formed since the other possible head-to-tail coupling was not allowed due to the extreme sensitivity of the reaction to steric hindrance [17]. Similarly, the thienyl derivative has shown the same behavior and produced a mixture of the two most stable cyclobutane derivatives in 1:1 ratio with an overall yield of 25 % [17].

Theoretically, several studies of the photochemical dimerization are available. For example, the photodimerization of cytosine by the CASSCF/CASPT2 method showed the most probable reaction along the potential energy hypersurface [21]. A mixture of two dimers formed by the irradiation of methyl urocanates by using PM3-RHF-CI semiempirical method which explains the regiochemical behavior and the interaction between the molecular orbital, LSOMO of the excited triplet state and the HOMO of the ground singlet state [22]. Also DFT and TD-DFT studies of methyl 3-(2-furyl)acrylate observed the regio- and stereoselectivity with only two of the eleven possible isomers being the most stable [20].

Obviously, the heterocyclic ring may play an important role on the regioselectivity and stereoselectivity behavior of photochemical dimerization of different heteroaryl acrylates [23–26]. In this study, DFT was used to study the regioselectivity and stereoselectivity of 3-heteroaryl (furyl, thiophyl, selenophyl and tellurophyl)-acrylates using B3LYP functional with different basis sets. All the intermediates and transition states were located along the potential energy surface. In addition, IR vibration frequencies, energetic parameters and molecular orbital analysis were analyzed for the most stable products.

Computational Details

Gaussian09 package was used for all theoretical calculations [27]. All the computations were based on DFT method with B3LYP functional in combination with two types of basis sets, 6-31+G(d,p) and 6-31G(d) [28]. The starting structures were built using GaussView and optimized to their corresponding ground states. The optimized structures were used to find the intermediates and the transition states along the reaction pathway. Geometry optimization was performed in default settings for geometry convergence, integration grid and electron density (SCF) convergence. Open-shell species calculations were done in a spin-restricted formalism. All molecular species were taken with a singlet spin multiplicity whether they have closed shells (reactants, products) or open shells of biradical nature (intermediates, transition states). Frequency calculations were used to verify that the structures of the reactants, intermediates and the products were at the ground state with no imaginary frequency. On the other hand, the transition states showed one imaginary frequency. Energetic, thermodynamic and spectroscopic parameters were calculated for all the intermediates and transition states along the reaction energy curve and were discussed in the results and discussion section.

Results and Discussion

The photochemical dimerization of methyl-3-(2-furyl) acrylate is shown in Scheme 3. It was experimentally shown that the reaction produced cis- and trans-isomers based on the distribution of the ester groups on the new formed cyclobutane ring. In addition, the reaction proceeds through head-to-head interaction in the triplet state following the energy transfer from the sensitizer molecule, benzophenone [18; 29].

Theoretically, DFT method was used to study the reaction pathway with 6-31G(d) basis set. Besides, the effect of replacing the furan ring by thiophene, selenophene and tellurophene on the reaction activation energy and the reaction final products was examined.

The coupling reaction of the reactant molecules involves the formation of two biradical intermediates, cis and trans in the triplet state after crossing the first transition state as shown in Fig. 1.

The energy difference between these intermediates is 1.59 kcal/mol which is close to the value obtained by D'Auria using AM1-UHF semiempirical method, 2.2 kcal/mol [22].

In the following reaction step, two biradicals go through a cyclization reaction to form the final corresponding dimers after crossing the second transition state, TS2, as shown in the reaction curve in Fig. 2. Table 1 shows the calculated electronic energies of all the possible dimers using two types of basis set, (6-31G+(d,p)) and (6-31g(d)). The reason behind using two types of basis set was to compare our results with those calculated by D'Aurai and to study the effect of the used basis set on the stability of the final products. Thermodynamic parameters such as ΔE (reaction energy), ΔH (reaction thermal enthalpy) and ΔG (Gibbs free energy) are collected in Table 1 and shown in Fig. 2.

In general, results obtained with the (6-31G+(d,p)) basis set are lower than those of the (6-31G(d)) basis set. However, both basis sets achieved the same most stable dimers: trans-anti-dimer, which represents entry 6 in Table 1, and cis-dimer, which is shown in entry 3. However, the order of the six dimers is different for the two types of basis sets.

It is worth noting that both basis sets showed identical geometry parameters for the final most stable derivative. Based on the previous results and considering that different basis sets gave different orders of stability, and due to the lack of experimental results, it is difficult to verify which basis set is able to give more accurate results, however, there is an agreement on the most stable product [20].

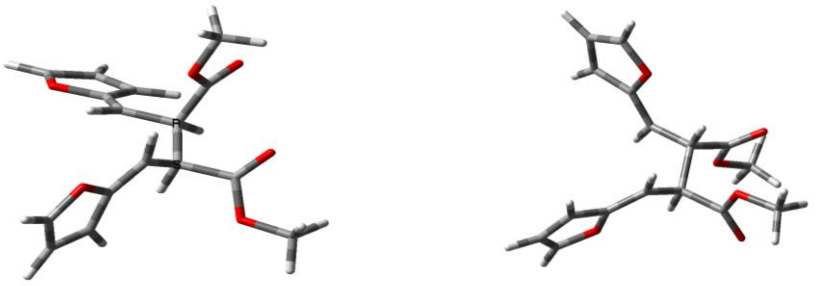

(cis) ΔE=31.39 kcal/mol **(trans) ΔE= 29.80 kcal/mol**

Fig. 1. The optimized geometries of the biradical intermediates using B3LYP/6-31+G(d,p) level of theory.

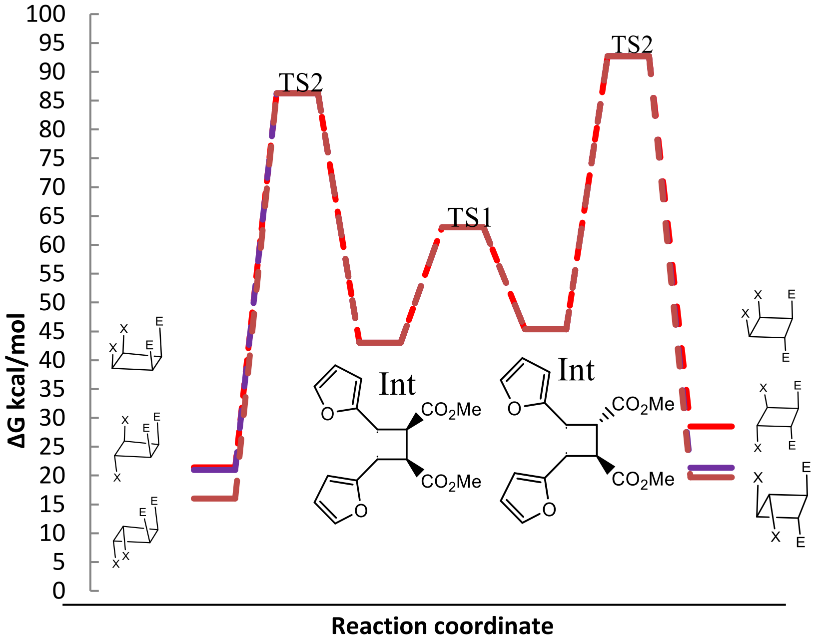

Fig. 2. The energy curve for the dimerization reaction with the biradical intermediates and all the possible cyclobutane derivatives, X= 2-furyl and E = $-CO_2CH_3$ using B3LYP/6-31+G(d,p) level of theory.

Table 1

The energy and thermodynamic parameters of the possible cyclobutane derivatives for the two types of basis sets using B3LYP functional in conjunction with 6-31+G(d,p) and 6-31G(d) basis sets.

Entry	Cyclobutane	ΔE (kcal/mol)		ΔH (kcal/mol)		ΔG (kcal/mol)	
		6-31G+(d,p)	6-31G(d)	6-31G+(d,p)	6-31G(d)	6-31G+(d,p)	6-31G(d)
1	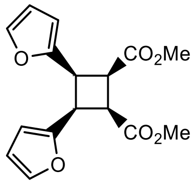	14.41	9.73	13.79	9.08	28.53	23.93
2	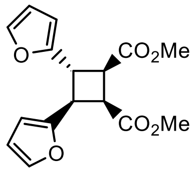	8.97	5.22	8.51	4.71	21.38	18.28
3	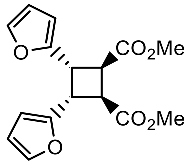	6.79	3.36	6.34	2.86	19.69	16.58
4	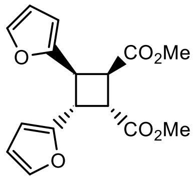	8.15	4.54	7.65	4.04	21.41	17.88
5	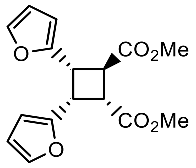	7.83	4.61	7.38	4.13	20.96	17.87
6	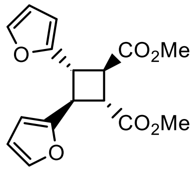	4.00	1.26	3.66	0.88	16.01	13.56

The optimized geometry:

In this study, we performed theoretical calculation for different heteroaryl acrylates (S, Se and Te) using DFT in the gas phase with 6-31g(d) basis set. The selected bond lengths, bond angles and torsion angles of the most stable dimer of all S, Se and Te derivatives are compared with O and listed in Table 2.

The C-C bond lengths of the formed cyclobutane ring are identical within a difference of ± 0.04 Å, while the C-H bond lengths have ± 0.01 Å difference. The differences of the bond angles of the most stable isomer of each derivative are within $\pm 1.39°$, $\pm 4.9°$ and $\pm 3.9°$ for the S, Se and Te, respectively comparative to the O-isomer.

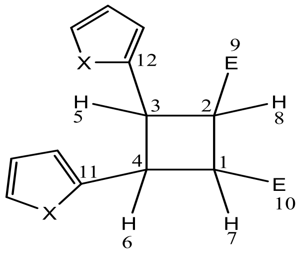

Table 2. The geometry parameters of the most stable dimer for the O, S, Se and Te derivatives using B3LYP/6-31+G(d,p) level of theory.

Definition	Isomers			
Bond/A°	O	S	Se	Te
C_1-C_2	1.56	1.56	1.55	1.55

C_1-C_4	1.56	1.56	1.57	1.57
C_1-H_7	1.09	1.09	1.09	1.09
C_2-C_9	1.51	1.51	1.51	1.51
C_3-C_{12}	1.48	1.49	1.50	1.50
Angle/degree				
$C_2C_1C_4$	88.4	88.3	87.3	88.2
$C_2C_1C_{10}$	118.7	118.5	119.8	116.8
$C_1C_2C_3$	88.2	88.3	89.4	88.6
$C_1C_2C_9$	118.8	118.5	122.5	116.6
$C_2C_3C_4$	87.5	87.8	86.2	87.6
$C_2C_3C_{12}$	119.4	120.8	117.3	121.3
$C_1C_4C_3$	88.1	88.0	88.2	88.2
Dihedral/degree				
$C_4C_1C_2C_9$	−143.2	−142.9	146.5	−138.7
$C_{10}C_1C_2C_3$	−143.9	−143.1	143.8	−138.7
$C_2C_1C_4C_{11}$	144.4	143.6	−152.4	144.0
$C_1C_2C_3C_{12}$	143.7	145.3	95.5	144.9

Thermodynamic parameters:

The calculated thermodynamic parameters are shown in Table 3, in which E represents the sum of the electronic and the zero-point energies, enthalpy H, which is the sum of the electronic and thermal enthalpy, Gibbs free energy G as the sum of the electronic and thermal free energy and entropy S.

The analysis of the results, based on comparing the thermodynamic parameters, shows that the most stable isomer is the one similar to 3-(2-furyl)acrylic acid, trans-anti-dimer isomer and the most stable cis isomer is entry 3 for O and Se isomer and entry 2 for S and Te.

Table 3

Energy and thermodynamic parameters of the possible cyclobutane derivatives for the O, S, Se and Te derivatives using B3LYP/6-31+G(d,p) level of theory.

Entry	Cyclobutane	derivatives	ΔE (kcal/mol)	ΔH_r (kcal/mol)	ΔG_r (kcal/mol)	ΔS (kcal/mol.K)
1	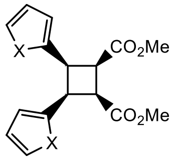	O	9.73	9.08	23.93	−49.81
		S	10.85	10.11	25.62	−52.04
		Se	1.28	0.44	17.26	−56.41
		Te	12.45	11.76	27.52	−52.84
2	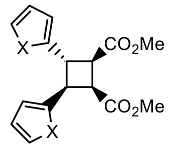	O	5.22	4.71	18.28	−45.51
		S	2.79	2.29	15.76	−45.21
		Se	2.60	1.96	16.92	−50.18
		Te	2.05	1.52	15.84	−48.02
3	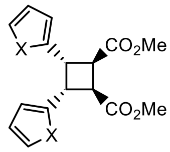	O	3.36	2.86	16.58	−46.01
		S	4.39	3.90	17.41	−45.34
		Se	−1.74	−2.31	12.58	−49.94
		Te	3.92	3.39	17.48	−47.27
4	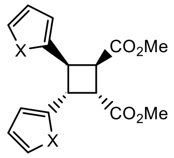	O	4.54	4.04	17.88	−46.43
		S	4.75	4.17	18.32	−47.48
		Se	0.05	-0.68	14.99	−52.56
		Te	2.65	2.04	16.76	−49.37
5	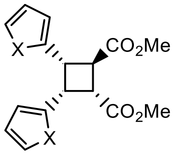	O	4.61	4.13	17.87	−46.10
		S	4.45	3.95	17.64	−45.91
		Se	−2.81	−3.41	11.88	−51.28
		Te	4.49	3.99	18.03	−47.10

6	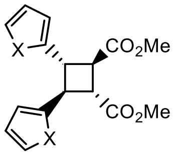	O	1.26	0.88	13.56	−42.52
		S	0.88	0.48	13.07	−42.23
		Se	−1.79	−2.18	11.17	−44.77
		Te	−2.14	−2.55	10.60	−44.10

Boundary Molecular Orbitals analysis (BMO)

Boundary molecular orbitals (BMO) analysis plays an important role in the study of electronic, optical and chemical properties [30]. The highest occupied molecular orbital (HOMO), which is the outer electron-containing orbital, can refer to an electron donor while the lowest unoccupied molecular orbital (LUMO), which contain free places to accept electrons, makes it an electron acceptor [31].

The molecular orbitals (HOMO and LUMO) of the most stable isomer for the O, S, Se and Te derivatives are shown in Table 4. The ionization potential is directly related to the energy of the HOMO (IP=-E_{HOMO}) and the LUMO is directly related to the electronic affinity

(EA=-E_{LUMO}). High value of E_{HOMO} shows the tendency of the compound to donate electrons to the acceptor compound with low energy, whereas the low value of E_{LUMO} shows that the compound prefers to accept electrons. The difference in energy between the HOMO and the LUMO is called the energy gap, which represents an important factor for the compound stability. A molecule with a high energy gap (ΔE_{gap} = E_{LUMO}-E_{HOMO}) is less polarizable and generally associated with high kinetic stability and low chemical reactivity [32].

Chemical hardness, η((IP-EA)/2), and global softness, S (1/η), refer to the resistance of a system to the change in its electron numbers. Generally, a soft molecule has a low η, while a hard molecule has a high value [33]. The electronegativity, χ ((IP+EA)/2) reflects the ability of a molecule not to release its electrons [16]. The overall electrophilicity index ω ($\mu^2/2\eta$) characterizes the electrophilic power of the molecule [34]. The global descriptors of reactivity for all isomers are listed in Table 5.

The global hardness of the isomers is decreased in the direction from O, S, Se and Te or as the size of the heteroatom or its electronegativity character increases. On the contrary, the global softness *S* increases in the direction from O to S, Se and Te. The electrophilicity power increases in the direction from O, through S and Se to Te. In particular, the isomer containing an oxygen atom has the lowest global electrophilicity *ω*. This compound has a wider energy gap among the others.

Table 4

The BMO (HOMO and LUMO) and their energies for the O, S, Se and Te most stable isomer using B3LYP/6-31+G(d,p) level of theory.

Str	HOMO	LUMO
O	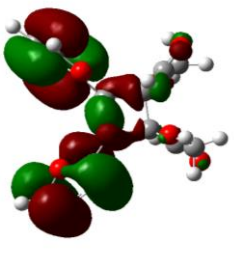 E= −0.31 eV	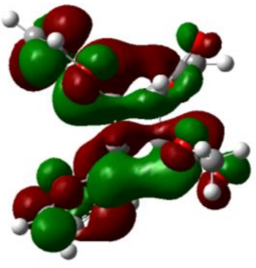 E= −0.15 eV
S	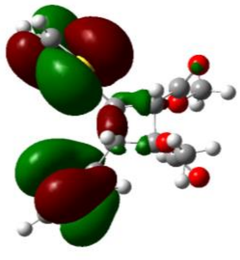 E= −0.31 eV	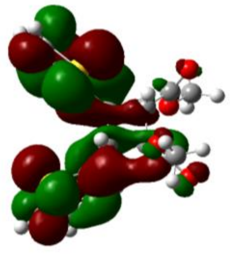 E= −0.14 eV

Se	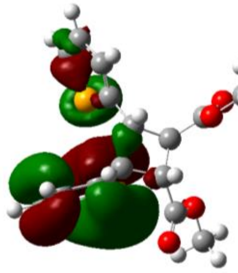 E= –0.26 eV	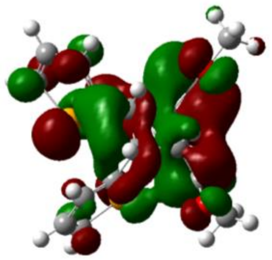 E= –0.14 eV
Te	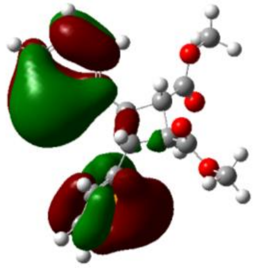 E= –0.28 eV	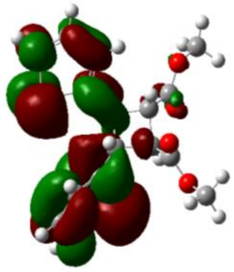 E= –0.18 eV

Table 5

The energy gap, IP, EA, hardness η, softness S, electronegativity and electrophilicity of the most stable isomer of the O, S, Se and Te derivatives using B3LYP/6-31+G(d,p) level of theory.

Parameters / Isomers	O	S	Se	Te
E_{gap}(kJ/mol)	15.44	13.51	11.58	9.65
IP kJ/mol	30.133	29.558	24.570	26.730
EA kJ/mol	14.088	14.848	13.111	16.976
η kJ/mol	8.022	7.355	5.730	4.877
S kcal/mol.K	0.125	0.136	0.175	0.205
χ kJ/mol	22.111	22.203	18.841	21.853
ω kJ/mol	30.469	33.514	30.975	48.960

IR vibrational frequencies

The vibrational frequencies for all the fundamental modes of the optimized O, S, Se and Te were computed using B3LYP method and 6–31g(d) basis set. As the molecule consists of 38 atoms, there are 108 fundamental modes of vibrations. The essential vibrational frequencies of compounds and the corresponding value of each vibration mode are summarized in Table 6.

The C–H stretching vibrations of the butane ring are observed in the region 3100–3000 cm^{-1}, however, for the current derivatives, the stretching vibrations appear between 3034–3153 cm^{-1}. The bands between 1089–117 cm^{-1} are assigned to the C-C ring stretching. The C1-C10 vibrations at 1286, 1284 and 1279 cm^{-1} are for the O, S and Se derivatives respectively.

The vibrations of the C3-C12 bond at 1279, 1232, 1227 and 1182 cm^{-1} are decreasing in the direction from O, S, Se and Te, respectively which may show the effect of the size of the heteroatom. The IR vibration spectrum for all derivatives is shown in Fig. 3. The scaling factor for the vibrational frequencies was calculated by Ünel et al., using the same basis set, and was 0.9522 [35]. The frequencies of the selected compounds were scaled by using derived scale factors.

Table 6

Essential vibration frequencies (cm^{-1}), Vibration frequencies (cm^{-1}) in *italic* after scaling, and IR intensities in parentheses of the most stable isomer of the O, S, Se and Te derivatives using B3LYP/6-31+G(d,p) level of theory.

Definition	O	S	Se	Te
C-C str	947.22 *901.94* (11.31)	955.11 *909.46* (5.2)	896.15 *853.32* (9.01)	966.61 *920.41* (8.20)
C-C str	955.93 *910.24* (12.69)	1011.8 *963.44* (1.97)	973.29 *926.76* (4.66)	994.97 *947.41* (22.37)
C-C str	1022.10 *973.24* (4.00)	1022.40 *973.53* (4.1)	979.15 *932.35* (9.47)	1004.47 *956.46* (5.03)
C-C str	1023.01 *947.11* (4.01)	1011.84 *963.47* (1.98)	915.53 *871.77* (10.74)	1034.47 *985.02* (1.61)
C-C Ring	1093.08 *1040.83* (1.30)	1089.04 *1036.98* (2.95)	1103.96 *1051.20* (3.80)	1117.81 *1064.39* (0.59)
C3-C12 str	1279.45 *1218.29* (14.03)	1232.87 *1173.94* (20.62)	1227.97 *1169.27* (6.72)	1182.38 *1125.86* (14.45)
C1-C10 str	1286.24 *1224.76* (477.56)	1284.31 *1222.92* (411.96)	1279.42 *1218.26* (323.12)	1374.13 *1308.45* (140.17)
C=C str	1644.30 *1565.70* (3.19)	1598.90 *1522.47* (0.9)	1599.40 *1522.95* (0.76)	1609.52 *1532.58* (0.59)
C=O str	1825.10 *1737.86* (200.45)	1826.31 *1739.01* (218)	1827.92 *1740.55* (249.35)	1816.65 *1729.81* (5.51)
C4-H6 str	3102.78 *2954.47* (0.30)	3089.40 *2941.73* (0.67)	3072.80 *2925.92* (8.21)	3034.43 *2889.38* (8.98)
C3-H5 str	3117.60 *2968.58* (3.96)	3102.60 *2954.30* (6.01)	3093.72 *2945.86* (16.10)	3069.29 *2922.58* (6.43)
C2-H8 str	3152.76 *3002.06* (10.73)	3135.01 *2985.15* (0.91)	3110.10 *2961.44* (5.15)	3127.24 *2977.79* (2.36)
C1-H7 str	3137.29 *2987.33* (1.77)	3150.80 *3000.19* (5.4)	3142.10 *2991.91* (5.61)	3141.22 *2991.07* (3.29)

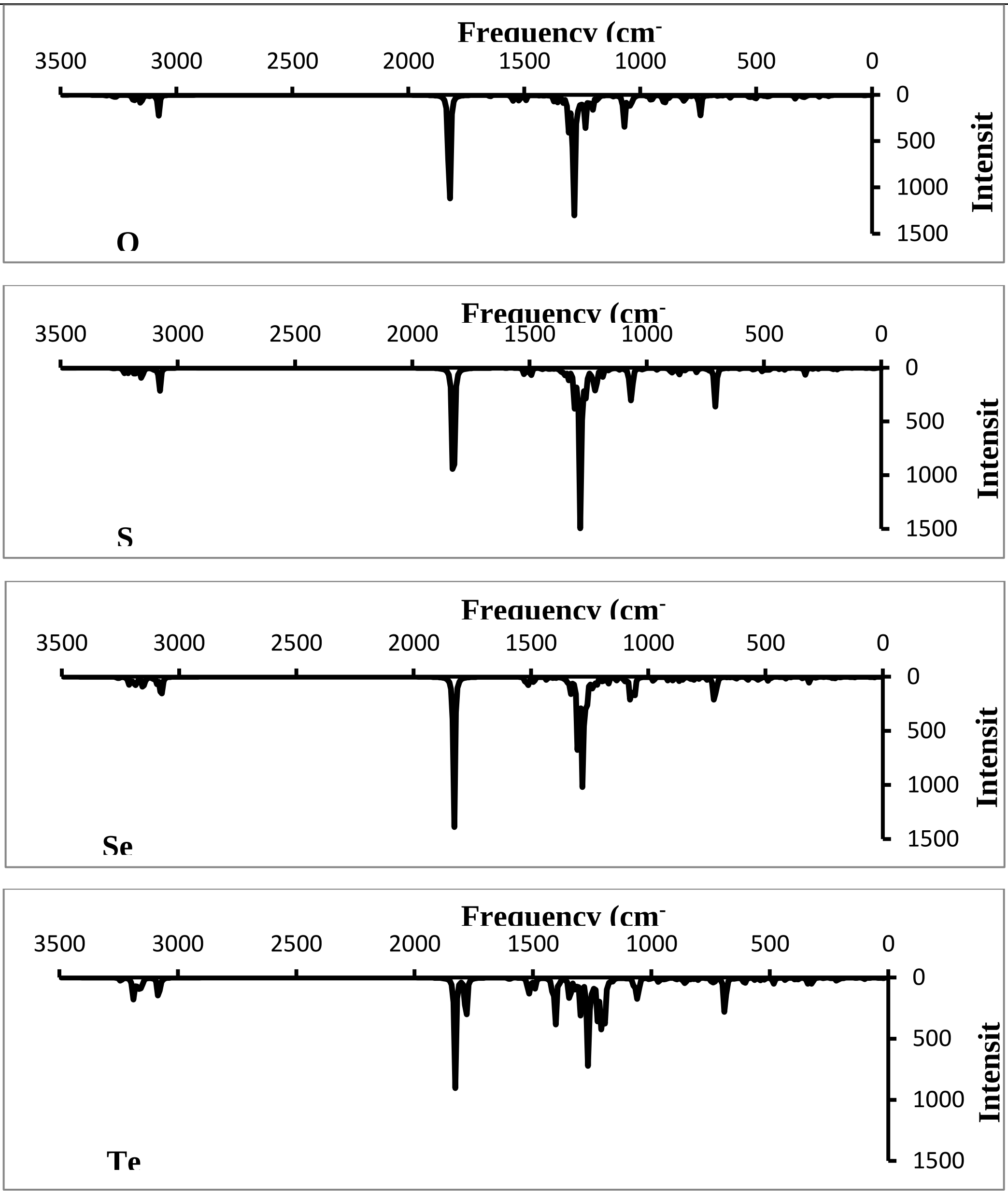

Fig. 3. IR spectra of the most stable isomer of the O, S, Se and Te derivatives using B3LYP/6-31+G(d,p) level of theory.

ELF topological analysis of reactants

The ELF establishes a direct quantitative connection between the electron density distribution and the chemical structure [36–43]. Herein, the reactivity of reactants in dimerization reactions is studied from the ELF topological analysis. The ELF localization domains of the reagents are given in Fig. 4.

The ELF topology of the reactant with O, S and Se shows the presence of two V(C1,C2) and V'(C1,C2) disynaptic basins having a total population of 3.39 e, 3.42 e and 3.43 e, respectively. The V(C1,C2) and V'(C1,C2) disynaptic basins represent the double bond electron density for the C-C bonding region. The total population of the electron density in the C-C double bond region increases in the direction from O, S to Se. However, only one V(C1,C2) disynaptic with the population of 3.60 e is shown for Te, associated with the underpopulated C–C double bond. It should be noted that the population of the electron density in the C-C double bonding region significantly increases on proceeding from O, S, Se onto Te.

After establishing the bonding pattern of the reagents, the atomic charge distribution of reactants was analyzed through NPA (Fig. 5). C1 and C2 carbon atoms of all reactants are negatively charged. The C1 carbon shows less negative charge than C2 carbon atom for all reactants. The charge of the carbon atom attached to the heterocycle becomes less negative in the direction from O, S, Se and Te.

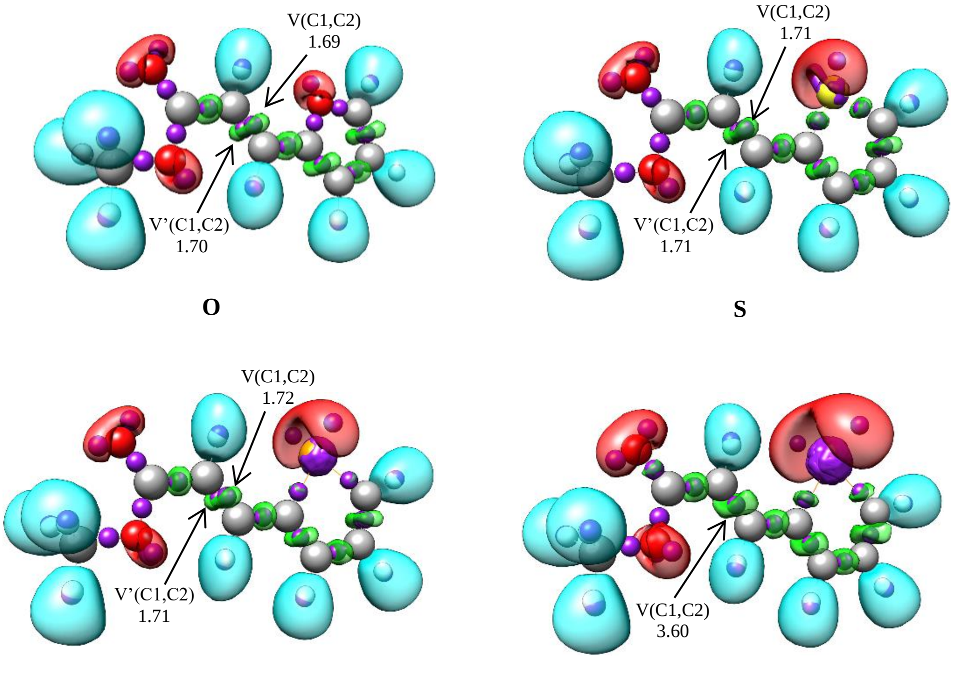

O **S**

Se **Te**

Fig. 4. B3LYP/6-31+G(d) calculated ELF localisation domains represented at an isosurface value of ELF = 0.80 of all reactants.

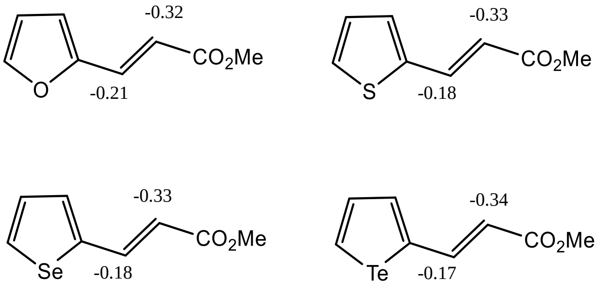

Fig. 5. B3LYP/6-31+G(d) calculated natural atomic charges, in average number of electrons e, of reactants.

Conclusion

In conclusion, we showed that the regio- and stereochemical behaviour of photochemical dimerization of the heterocyclic substituted alkenes bearing electron withdrawing groups can be predicted on the basis of these photophysical and chemical properties. The reaction proceeds through head-to-head interaction, which is sensitized from the excited triplet state. The product bearing the ester functions in anti-configuration is more stable than the other one. Isomer 6, is the most stable isomer in the case of O, S and Te, while for the Se derivative, isomer 5 is the most stable. The formation of the more stable isomers can be understood on the basis of the different stability of the biradical intermediates and the transition state energy of the ring-closure reaction.

Bibliography

[1] Salim H. M. In Mechanism and Thermodynamic Parameters of Paternò-Büchi Reaction of Benzene and Furan: DFT Study / H. M. Salim, H. H. Abdallah, P. Ramasami // International Conference on Advanced Science and Engineering (ICOASE), IEEE. – 2018. – P. 415–419.

[2] Bach T. Photochemical reactions as key steps in natural product synthesis / T. Bach, J. P. Hehn // Angewandte Chemie International Edition. – 2011. – Vol. 50, N 5. – P. 1000–1045.

[3] Namyslo J. C. The application of cyclobutane derivatives in organic synthesis / J. C. Namyslo, D. E. Kaufmann // Chemical reviews. – 2003. – Vol. 103, N 4. – P. 1485–1538.

[4] Lee-Ruff E. Enantiomerically pure cyclobutane derivatives and their use in organic synthesis / E. Lee-

Ruff, G. Mladenova // Chemical reviews. – 2003. – Vol. 103, N 4. – P. 1449–1484.

[5] Østby R. B. Syntheses of 3-, 4-and 5-membered carbocycles: new methodology on old methods / R. B. Østby. – 2020. https://hdl.handle.net/11250/2687783

[6] Gutekunst W. R. Total synthesis and structural revision of the piperarborenines via sequential cyclobutane C–H arylation / W. R. Gutekunst, P. S. Baran // Journal of the American Chemical Society. – 2011. – Vol. 133 N 47. – P. 19076–19079.

[7] Hansen T. Naturally Occurring Cyclobutanes in Organic Synthesis: Theory and Applications / T. Hansen, Y. Stenstrøm – Elsevier, Oxford, UK, 2001. – 276 p.

[8] Dembitsky V. M. Bioactive cyclobutane-containing alkaloids / V. M. Dembitsky // Journal of natural medicines. – 2008. – Vol. 62, N 1. – P. 1–33.

[9] Cyclobutane-containing alkaloids: origin, synthesis, and biological activities / A. Sergeiko, V. V. Poroikov, L. O. Hanuš, V. M. Dembitsky // The open medicinal chemistry journal. – N 2. – P. 26.

[10] Crack healing in polymeric materials via photochemical [2+2] cycloaddition / C.-M. Chung, Y.-S. Roh, S.-Y. Cho, J.-G. Kim // Chemistry of Materials. – 2004. – Vol. 16, N 21. – P. 3982–3984.

[11] Alcaide B. Exploiting [2+2] cycloaddition chemistry: achievements with allenes / B. Alcaide, P. Almendros, C. Aragoncillo // Chemical Society Reviews. – 2010. – Vol. 39, N 2. – P. 783–816.

[12] Ciamician G. (1902). Giacomo ciamician und P. silber: chemische lichtwirkungen / G. Ciamician // Chem Ges. – 1902. – N 35. – P. 4128–4131.

[13] Wondraczek H. (2012). Water soluble photoactive cellulose derivatives: synthesis and characterization of mixed 2-[(4-methyl-2-oxo-2H-chromen-7-yl)oxy] acetic acid–(3-carboxypropyl) trimethylammonium chloride esters of cellulose / H. Wondraczek, A. Pfeifer, T. Heinze // Cellulose – 2012. – Vol. 19, N 4. – P. 1327–1335.

[14] Hoffmann N. Photochemical reactions of aromatic compounds and the concept of the photon as a traceless reagent / N. Hoffmann // Photochemical & Photobiological Sciences. – 2012. – Vol. 11, N 11. – P. 1613–1641.

[15] Photocycloaddition in liquid ethyl cinnamate and in ethyl cinnamate glasses. The photoreaction as a probe into the micromorphology of the solid / P. Egerton, E. Hyde, J. Trigg [et al.] // Journal of the American Chemical Society. –1981. – Vol. 103, N 13. – P. 3859–3863.

[16] Bolt J. Solid state photodimerization of surfactant esters of cinnamic acid / J. Bolt, F. H. Quina, D. G. Whitten // Tetrahedron Letters. – 1976. – Vol. 17, N 30. – P. 2595–2598.

[17] D'Auria M. Photochemical dimerization of methyl 2-furyl-and 2-thienylacrylate and related compounds in solution / M. D'Auria, G. Piancatelli, A. Vantaggi // Journal of the Chemical Society, Perkin Transactions 1. – 1990. – Vol. 11. – P. 2999–3002.

[18] D'Auria M. Regio-and stereochemical control in the photodimerization of methyl 3-(2-furyl) acrylate / M. D'Auria // Heterocycles. – 1996. – Vol. 5, N 43. – P. 959–968.

[19] D'Auria M. Photochemical behaviour of furylidene carbonyl compounds / M. D'Auria, A. D'Annibale, T. Ferri // Tetrahedron. – 1992. – Vol. 48, N 42. – P. 9323–9336.

[20] D'Auria M. A DFT Study of the Photochemical Dimerization of Methyl 3-(2-Furyl) acrylate and Allyl Urocanate / M. D'Auria // Molecules. – 2014. – Vol. 19, N 12. – P. 20482–20497.

[21] On the photoproduction of DNA/RNA cyclobutane pyrimidine dimers / I. González-Ramírez, D. Roca-Sanjuán, T. Climent [et al.] // Theoretical Chemistry Accounts. – 2011. – Vol. 128, N 4. – P. 705–711.

[22] (2002). The photochemical dimerization of 3-heteroaryl-acrylates / M. D'Auria, L. Emanuele, V. Esposito, R. Racioppi // Arkivoc. – 2002. – N 11. – P. 65–78.

[23] Salim H. A. M. In Stereoselectivity and regioselectivity of the cycloaddition dimerization of allyl 3-(2-pyridyl) acrylate and allyl 3-(2-pyrryl) acrylate: DFT Calculations / H. A. M. Salim, H. H. Abdallah, P. Ramasami // IOP Conference Series: Materials Science and Engineering, IOP Publishing: 2018. – 2018. – P. 012049.

[24] Mechanistic study of the [2+2] cycloaddition reaction of cyclohexenone and its derivatives with vinyl acetate / H. A. Mohammad-Salim, H. H. Abdallah, K. R. Maiyelvaganan [et al.] // Theoretical Chemistry Accounts. – 2020. – Vol. 139, N 2. – P. 1–11.

[25] Mohammad-Salim H. A. Theoretical Study of the [4+2] Cycloaddition Reaction of Trifluoroethylene with Five-membered Chalcogens Heterocyclic Compounds / H. A. Mohammad-Salim, H. H. Abdallah // ARO-The Scientific Journal of Koya University. – 2019. – Vol. 7, N 2. – P. – 9.

[26] Mohammad Salim H. Theoretical Study for the [2+2] Cycloaddition Reaction Mechanism of Ketenes and their Derivatives / H. Mohammad Salim, H. Abdallah // Oriental Journal Of Chemistry. – 2019. – Vol. 35. – P. 1550–1556.

[27] Gaussian 09, Revision D. 01 / Frisch M., Trucks G., Schlegel, H. [et al.]. – Gaussian. Inc., Wallingford CT, 2009.

[28] Parr R. G. W. Yang. Density functional theory of atoms and molecules / R. G. W. Yang Parr // Oxford University Press. – 1989. – N 1. – P. 989.

[29] D'Auria M. Photochemical dimerization of esters of urocanic acid / M. D'Auria, R. Racioppi // Journal of Photochemistry and Photobiology A: Chemistry. – 1998. – Vol. 112, N 2-3. – P. 145–148.

[30] Woodward R. HR The Conservation of Orbital Symmetry / R. Woodward, R. Hoffmann. – Verlag Chemie. Weinheim/Deerfield Beach, 1970. – 184 p.

[31] Gece G. The use of quantum chemical methods in corrosion inhibitor studies / G. Gece // Corrosion science. – 2008. – Vol. 50, N 11. – P. 2981–2992.

[32] Sinha L. Spectroscopic analysis and first-order hyperpolarisability of 3-benzoyl-5-chlorouracil by first principles / L. Sinha, O. Prasad, V. Narayan, S. Shukla // J. Mol. Simul. – 2011. – N 37. – P. 153.

[33] Pearson R. G. Hard and Soft Acids and Bases / R. G. Pearson // Journal of the American Chemical Society. – 1963. – Vol. 85, N 22. – P. 3533–3539.

[34] Molecular basis of DNA photodimerization: Intrinsic production of cyclobutane cytosine dimers / D. Roca-Sanjuán, G. Olaso-González, I. Gonzalez-Ramirez [et al.] // Journal of the American Chemical Society. – 2008. – Vol. 130, N 32. – P. 10768–10779.

[35] Scale factor database for the vibration frequencies calculated in M06-2X, one of the DFT methods / Y. Ünal, W. Nassif, B. C. Özaydin, K. Sayin // Vibrational Spectroscopy. – 2021. – Vol. 112. – P. 103189.

[36] A molecular electron density theory study for [3+2] cycloaddition reactions of 1-pyrroline-1-oxide with disubstituted acetylenes leading to bicyclic 4-isoxazolines / H. A. Mohammad-Salim, N. Acharjee, L. R. Domingo, H. H. Abdallah // International Journal of Quantum Chemistry. – 2021. – Vol. 121, N 5. – e26503.

[37] Unveiling the high regioselectivity and stereoselectivity within the synthesis of spirooxindolenitropyrrolidine: A molecular electron density theory perspective / N. Acharjee, H. A. Mohammad-Salim, M. Chakraborty [et al.] // Journal of Physical Organic Chemistry. – 2021. – e4189.

[38] Mohammad-Salim H. A. Understanding the Reactivity of C-Cyclopropyl-N-Methylnitrone Participating in [3+2] Cycloaddition Reactions Towards Styrene with a Molecular Electron Density Theory Perspective / H. A. Mohammad-Salim // Journal of the Mexican Chemical Society. – 2021. – Vol. 65, N 1. – P. 129–140.

[39] Mohammad-Salim H. A. Insights into the mechanism and regioselectivity of the [3+2] cycloaddition reactions of cyclic nitrone to nitrile functions with a molecular electron density theory perspective / H. A. Mohammad-Salim, N. Acharjee, H. H. Abdallah // Theoretical Chemistry Accounts. – 2021. – Vol. 140, N 1. – P. 1–14.

[40] A molecular electron density theory study for [3+2] cycloaddition reactions of N-benzylcyclohexylnitrone with methyl-3-butenoate. / H. A. Mohammad-Salim, H. A. Basheer, H. H. Abdallah [et al.] // New Journal of Chemistry. – 2021. – Vol. 45, N 1. – P. 262–267.

[41] Domingo L. R. Understanding the Reactivity of Trimethylsilyldiazoalkanes Participating in [3+2] Cycloaddition Reactions towards Diethylfumarate with a Molecular Electron Density Theory Perspective. / L. R. Domingo, N. Acharjee, H. A. Mohammad-Salim // Organics. – 2020. – Vol. 1, N 1.

[42] Insights into the mechanism and regiochemistry of the 1,3-dipolar cycloaddition reaction between benzaldehyde and diazomethane / K. Abbiche, H. Mohammad-Salim, M. Salah [et al.] // Theor. Chem. Acc. – 2020. – Vol. 139, N 9. – P. 148.

[43] The Theoretical Study on the Mechanism of [3+2] Cycloaddition Reactions between α, β-unsaturated Selenoaldehyde with Nitrone and with Nitrile Oxide / H. Mohammad-Salim, R. Hassan, H. H. Abdallah, M. Oftadeh // Journal of the Mexican Chemical Society. – 2020. – Vol. 64, N 2. – P. 147–164.

References

[1] Salim, H. M., Abdallah, H. H., Ramasami, P. (2018). In Mechanism and Thermodynamic Parameters of Paternò-Büchi Reaction of Benzene and Furan: DFT Study. *International Conference on Advanced Science and Engineering (ICOASE), IEEE: 2018*, 415–419.

[2] Bach, T., Hehn, J. P. (2011). Photochemical reactions as key steps in natural product synthesis. *Angewandte Chemie International Edition, 50* (5), 1000–1045.

[3] Namyslo, J. C., Kaufmann, D. E. (2003). The application of cyclobutane derivatives in organic synthesis. *Chemical reviews, 103* (4), 1485–1538.

[4] Lee-Ruff, E., Mladenova, G. (2003). Enantiomerically pure cyclobutane derivatives and their use in organic synthesis. *Chemical reviews, 103* (4), 1449–1484.

[5] Østby, R. B. (2020). Syntheses of 3-, 4-and 5-membered carbocycles: new methodology on old methods. https://hdl.handle.net/11250/2687783

[6] Gutekunst, W. R. Baran, P. S. (2011). Total synthesis and structural revision of the piperarborenines via sequential cyclobutane C–H arylation. *Journal of the American Chemical Society, 133* (47), 19076–19079.

[7] Hansen, T., Stenstrøm, Y. (2001). Naturally Occurring Cyclobutanes in Organic Synthesis: Theory and Applications. *Elsevier, Oxford, UK.*

[8] Dembitsky, V. M. (2008). Bioactive cyclobutane-containing alkaloids. *Journal of natural medicines*, *62*(1), 1–33.

[9] Sergeiko, A., Poroikov, V. V., Hanuš, L. O., Dembitsky, V. M. (2008). Cyclobutane-containing alkaloids: origin, synthesis, and biological activities. *The open medicinal chemistry journal*, *2*, 26.

[10] Chung, C.-M., Roh, Y.-S., Cho, S.-Y., Kim, J.-G. (2004). Crack healing in polymeric materials via photochemical [2+2] cycloaddition. *Chemistry of Materials*, *16*(21), 3982–3984.

[11] Alcaide, B., Almendros, P., Aragoncillo, C. (2010). Exploiting [2+2] cycloaddition chemistry: achievements with allenes. *Chemical Society Reviews, 39*(2), 783–816.

[12] Ciamician, G. (1902). Giacomo ciamician und P. silber: chemische lichtwirkungen. *Chem Ges*, *35*, 4128–4131.

[13] Wondraczek, H., Pfeifer, A., Heinze, T. (2012). Water soluble photoactive cellulose derivatives: synthesis and characterization of mixed 2-[(4-methyl-2-oxo-2H-chromen-7-yl)oxy] acetic acid–(3-carboxypropyl) trimethylammonium chloride esters of cellulose. *Cellulose*, *19* (4), 1327–1335.

[14] Hoffmann, N. (2012). Photochemical reactions of aromatic compounds and the concept of the photon as a traceless reagent. *Photochemical & Photobiological Sciences*, *11*(11), 1613–1641.

[15] Egerton, P., Hyde, E., Trigg, J., Payne, A., Beynon, P., Mijovic, M., Reiser, A. (1981). Photocycloaddition in liquid ethyl cinnamate and in ethyl cinnamate glasses. The photoreaction as a probe into the micromorphology of the solid. *Journal of the American Chemical Society*, *103*(13), 3859–3863.

[16] Bolt, J., Quina, F. H., Whitten, D. G. (1976). Solid state photodimerization of surfactant esters of cinnamic acid. *Tetrahedron Letters*, *17*(30), 2595–2598.

[17] D'Auria, M., Piancatelli, G., Vantaggi, A. (1990). Photochemical dimerization of methyl 2-furyl-and 2-thienylacrylate and related compounds in solution. *Journal of the Chemical Society, Perkin Transactions 1*, (11), 2999–3002.

[18] D'Auria, M. (1996). Regio-and stereochemical control in the photodimerization of methyl 3-(2-furyl) acrylate. *Heterocycles, 5* (43), 959–968.

[19] D'Auria, M., D'Annibale, A., Ferri, T. (1992). Photochemical behaviour of furylidene carbonyl compounds. *Tetrahedron, 48*(42), 9323–9336.

[20] D'Auria, M. (2014). A DFT Study of the Photochemical Dimerization of Methyl 3-(2-Furyl) acrylate and Allyl Urocanate. *Molecules, 19*(12), 20482–20497.

[21] González-Ramírez, I., Roca-Sanjuán, D., Climent, T., Serrano-Pérez, J. J., Merchán, M., Serrano-Andrés, L. (2011). On the photoproduction of DNA/RNA cyclobutane pyrimidine dimers. *Theoretical Chemistry Accounts, 128* (4), 705–711.

[22] D'Auria, M., Emanuele, L., Esposito, V., Racioppi, R. (2002). The photochemical dimerization of 3-heteroaryl-acrylates. *Arkivoc, 11*, 65–78.

[23] Salim, H. A. M., Abdallah, H. H., Ramasami, P. (2018). In Stereoselectivity and regioselectivity of the cycloaddition dimerization of allyl 3-(2-pyridyl) acrylate and allyl 3-(2-pyrryl) acrylate: DFT Calculations, *IOP Conference Series: Materials Science and Engineering, IOP Publishing: 2018*, 012049.

[24] Mohammad-Salim, H. A., Abdallah, H. H., Maiyelvaganan, K. R., Prakash, M., Hochlaf, M. (2020). Mechanistic study of the [2+2] cycloaddition reaction of cyclohexenone and its derivatives with vinyl acetate. *Theoretical Chemistry Accounts, 139* (2), 1–11.

[25] Mohammad-Salim, H. A., Abdallah, H. H. (2019). Theoretical Study of the [4+2] Cycloaddition Reaction of Trifluoroethylene with Five-membered Chalcogens Heterocyclic Compounds. *ARO-The Scientific Journal of Koya University, 7*(2), 9. doi:10.14500/aro.10575

[26] Mohammad Salim, H., Abdallah, H. (2019). Theoretical Study for the [2+2] Cycloaddition Reaction Mechanism of Ketenes and their Derivatives. *Oriental Journal Of Chemistry, 35*, 1550–1556. doi:10.13005/ojc/350512

[27] Frisch, M., Trucks, G., Schlegel, H., Scuseria, G., Robb, M., Cheeseman, J., Scalmani, G., Barone, V., Mennucci, B., Petersson, G. (2009). Gaussian 09, Revision D. 01, 2009, Gaussian. *Inc., Wallingford CT*.

[28] Parr, R. G. W. Yang (1989). Density functional theory of atoms and molecules. *O xford University Press, 1*, 989.

[29] D'Auria, M., Racioppi, R. (1998). Photochemical dimerization of esters of urocanic acid. *Journal of Photochemistry and Photobiology A: Chemistry, 112* (2-3), 145–148.

[30] Woodward, R., Hoffmann, R. (1970). HR The Conservation of Orbital Symmetry. *Verlag Chemie. Weinheim/Deerfield Beach*.

[31] Gece, G. (2008). The use of quantum chemical methods in corrosion inhibitor studies. *Corrosion science, 50*(11), 2981–2992.

[32] Sinha, L., Prasad, O., Narayan, V., Shukla, S. (2011). Spectroscopic analysis and rst-order hyperpolarisability of 3-benzoyl-5-chlorouracil by rst principles. *J Mol Simul, 37*, 153.

[33] Pearson, R. G. (1963). Hard and Soft Acids and Bases. *Journal of the American Chemical Society, 85*(22), 3533–3539. doi:10.1021/ja00905a001

[34] Roca-Sanjuán, D., Olaso-González, G., Gonzalez-Ramirez, I., Serrano-Andrés, L., Merchán, M. (2008). Molecular basis of DNA photodimerization: Intrinsic production of cyclobutane cytosine dimers. *Journal of the American Chemical Society, 130*(32), 10768–10779.

[35] Ünal, Y., Nassif, W., Özaydin, B. C., Sayin, K. (2021). Scale factor database for the vibration frequencies calculated in M06-2X, one of the DFT methods. *Vibrational Spectroscopy, 112*, 103189.

[36] Mohammad-Salim, H. A., Acharjee, N., Domingo, L. R., Abdallah, H. H. (2021). A molecular electron density theory study for [3+2] cycloaddition reactions of 1-pyrroline-1-oxide with disubstituted acetylenes leading to bicyclic 4-isoxazolines. *International Journal of Quantum Chemistry, 121*(5), e26503.

[37] Acharjee, N., Mohammad-Salim, H. A., Chakraborty, M., Rao, M. P., Ganesh, M. (2021). Unveiling the high regioselectivity and stereoselectivity within the synthesis of spirooxindolenitropyrrolidine: A molecular electron density theory perspective. *Journal of Physical Organic Chemistry,* e4189.

[38] Mohammad-Salim, H. A. (2021). Understanding the Reactivity of C-Cyclopropyl-N-Methylnitrone Participating in [3+2] Cycloaddition Reactions Towards Styrene with a Molecular Electron Density Theory Perspective. *Journal of the Mexican Chemical Society, 65* (1), 129–140. https://doi.org/10.29356/jmcs.v65i1.1437

[39] Mohammad-Salim, H. A., Acharjee, N., Abdallah, H. H. (2021). Insights into the mechanism and regioselectivity of the [3+2] cycloaddition reactions of cyclic nitrone to nitrile functions with a molecular electron density theory perspective. *Theoretical Chemistry Accounts, 140*(1), 1–14.

[40] Mohammad-Salim, H. A., Basheer, H. A., Abdallah, H. H., Zeroual, A., Jamil, L. A. (2021). A molecular electron density theory study for [3+2] cycloaddition reactions of N-benzylcyclohexylnitrone with methyl-3-butenoate. *New Journal of Chemistry, 45*(1), 262–267.

[41] Domingo, L. R., Acharjee, N., Mohammad-Salim, H. A. (2020). Understanding the Reactivity of Trimethylsilyldiazoalkanes Participating in [3+2] Cycloaddition Reactions towards Diethylfumarate with a Molecular Electron Density Theory Perspective. *Organics, 1*(1). doi:10.3390/org1010002

[42] Abbiche, K., Mohammad-Salim, H., Salah, M., Mazoir, N., Zeroual, A., El Alaoui El Abdallaoui, H., El Hammadi, A., Hilali, M., Abdallah, H. H., Hochlaf, M.. (2020). Insights into the mechanism and regiochemistry of the 1,3-dipolar cycloaddition reaction between benzaldehyde and diazomethane. *Theor. Chem. Acc., 139*(9), 148. doi:10.1007/s00214-020-02662-4

[43] Mohammad-Salim, H., Hassan, R., Abdallah, H. H., Oftadeh, M. (2020). The Theoretical Study on the Mechanism of [3+ 2] Cycloaddition Reactions between α, β-unsaturated Selenoaldehyde with Nitrone and with Nitrile Oxide. *Journal of the Mexican Chemical Society*, *64* (2), 147–164. http://dx.doi.org/10.29356/jmcs.v64i2.1111